ELSEVIER

Materials Science and Engineering A 395 (2005) 102–109

MATERIALS SCIENCE & ENGINEERING A

www.elsevier.com/locate/msea

Evaluation of bendability of sheet metals using void coalescence models

A.R. Ragab*, Ch. A. Saleh

Department of Mechanical Design and Production, Faculty of Engineering, Cairo University, Giza 12613, Egypt

Received 2 August 2004; received in revised form 1 December 2004; accepted 3 December 2004

Abstract

Bendability of sheet metals often refers to the ratio of the minimum bend radius to the sheet thickness at which the bending process is accomplished successfully. Failure here denotes the occurrence of shear bands, localized necking, cracks or ultimately fracture. The conditions to prevent these types of failures are directly related to the exhaustion of tensile ductility of the outer material fiber at the convex side of the bent sheet. In the present work the bendability of sheet metals are predicted by considering two types of possible failure conditions; namely shear band formation or micro-necking within the material ligaments between neighboring voids. Such analysis is based on assuming a material with an initial void fraction together with a formulation for the laws governing void growth in volume and evolution in shape for porous solids. The results obtained display the effects of hardening as well as anisotropy. The predicted bendability plotted versus ductility is compared favorably with experimental evidence from the literature for various sheet metals.

Keywords: Bendability; Ductile failure; Void coalescence

1. Introduction

Bending is a very common forming process to change sheets and plates into structural shapes. In addition bending occurs as a part of several forming operations e.g.deep drawing. The bendability of sheet metals often refers to the minimum die radius over which a sheet with a given thickness can be bent successfully without defects [1]. The process is limited by the occurrence of shear bands, thickness inhomogeneties, microcracks, and ultimately fracture on the convex surface of the bent sheet. These defects depend phenomenologically on width to thickness ratio, edge conditions, cold working, hardening and anisotropy; all affecting ductility of the bent sheet. Most of these factors are related to the microstructural characteristics of the sheet metal such as the presence of inclusions, stringers, voids and fibering. However the prediction of bendability has generally relied on specifying the reduction of area in a tension test [2] without much insight for the effect of each one of the above parameters. Some investigators [3,4] have included the effect of hardening and anisotropy on the prediction of bendability which is still expressed in terms of the measured reduction of area in tension.

In the present investigation, it is intended to correlate bendability to ductility of sheet metals. Both parameters are to be predicted from analyzing ductile failure due to growth and coalescence of initially existing voids in the sheet material. This analysis will rely on description of plastic deformation for voided solids coupled with selected ductile fracture criteria.

2. Determination of minimum bend radius

Consider a wide isotropic sheet in which a cylindrical bent region is flanked by flat sheet. For small radius bends the displacement of the neutral axis in bending is significant and the solution by Hoffman and Sachs [5] has been employed by most investigators [2,4]. The nonlinear strain distribution gives at the outer tensile fiber

$$\varepsilon_1 = \ln\left(\frac{R_o}{R_n}\right) = \ln\left(\frac{R_i + t_o}{R_n}\right) \quad (1)$$

* Corresponding author. Tel.: +20 2 5703620; fax: +20 2 5703620.
E-mail address: a.r.ragab@link.net (A.R. Ragab).

0921-5093/$ – see front matter © 2004 Elsevier B.V. All rights reserved.
doi:10.1016/j.msea.2004.12.011

Nomenclature

A_f	reduction in area at fracture
b_1, b_2	half length of axis of a shperoidal void and surrounding matrix material transverse to maximum principal stress, respectively
f	void volume fraction
m	exponent in non-quadratic anisotropic yield function
n	strain-hardening exponent
q_1, q_2	semi-empirical parameters in Gurson–Tvergaard yield function
$\bar{r}$	normal anisotropy parameter
R_i, R_o, R_n	inner, external and neutral bending radii respectively
t_o	thickness of bent sheet metal

Greek letters

α	stress ratio σ_2/σ_1
ε_f	fracture strain
ε_i	strain ($i = 1, 2, 3$)
ε_v	volumetric strain
$\bar{\varepsilon}$, $\bar{\varepsilon}_M$	effective macroscopic and effective matrix strain respectively
λ_1	aspect ratio of a spheroidal void
σ_i	stress ($i = 1, 2, 3$)
$\bar{\sigma}$, $\bar{\sigma}_M$	effective macroscopic and effective matrix stress respectively

Subscripts

f	fracture
i	initial
l	ligament
M	matrix

where

$$R_n = \sqrt{R_o R_i} = \sqrt{(R_i + t_o) R_i}$$

Bendability of the sheet is exhausted when cracks or shear bands on the convex surface appear. At this moment this strain ε_1 attains its limiting value ε_f at failure. In terms of the reduction in area at failure of a tensile rod

$$\boldsymbol{\varepsilon}_f = \ln\left[\frac{1}{1 - \boldsymbol{A}_f}\right] \tag{2}$$

Combining expressions (1) and (2) yields the bendability of the sheet expressed by the ratio $(R_i/t_o)_{min}$ [2] as

$$\left(\frac{R_i}{t_o}\right)_{min} = \frac{(1 - \boldsymbol{A}_f)^2}{2A_f - \boldsymbol{A}_f^2} \tag{3}$$

This expression is extended to sheets with normal anisotropy $\bar{r}$ by Wang et al. [3] such that

$$\left(\frac{R_i}{t_o}\right)_{min} = \frac{(1 - \boldsymbol{A}_f)^{2/F}}{1 - (1 - \boldsymbol{A}_f)^{2/F}} \tag{4}$$

where

$$F = \frac{[2(1 + \bar{r})]^{1/m}}{2}[1 + (1 + 2\bar{r})^{1/(1-m)}]^{(m-1)/m}$$

and $m = 1 + \bar{r}$ for $\bar{r} < 1$ and m = 2 for $\bar{r} > 1$ [6].

Note that m is an exponent characterizing the non-quadratic Hill yield function [7] for sheet metals possessing normal anisotropy such that the effective macroscopic stress is given by

$$\bar{\sigma} = \left\{\frac{1}{2(1 + \bar{r})}[|2\sigma_3 - \sigma_1 - \sigma_2|^m + (1 + 2\bar{r})\,|\sigma_1 - \sigma_2|^m]\right\}^{1/m} \tag{5}$$

A different bendability criterion based on the attainment of maximum bending moment has been derived by Leu [4] as

$$\left(\frac{R_i}{t_o}\right)_{min} = \frac{1}{2}\left[\frac{1}{\exp(nF_1/2)} - 1\right] - \frac{1}{2} \tag{6}$$

where

$$F_1 = \frac{1 + \bar{r}}{\sqrt{1 + 2\bar{r}}}$$

Leu established his bendability criterion using Hill's quadratic yield function for orthotropic anisotropy as given by [8]

$$\bar{\sigma} = \sqrt{\frac{3}{2}}\left[\frac{r_0(\sigma_2 - \sigma_3)^2 + r_{90}(\sigma_3 - \sigma_1)^2 + r_0 r_{90}(\sigma_1 - \sigma_2)^2}{r_0 + r_{90} + r_0 r_{90}}\right]^{1/2} \tag{7}$$

where r_0 = H/G, r_{90} = H/F and $\bar{r} = (r_0 + r_{90})/2$ are determined from tensile test-pieces cut along and transverse to the rolling direction respectively. In the above bendability criteria (3) and (4), ε_f and hence A_f customarily are determined from tensile testing. The present work devotes the proceeding sections to state the governing equations required to estimate the fracture strains and hence bendability from micro mechanical data of the sheet metal. These equations are based on assuming that the sheet material initially contains voids which grow and either form shear bands or coalesce leading to ductile fracture.

3. Void growth laws

Void growth laws used in the present analysis rely on a yield function for cavitated solids due to Gurson–Tvergaard

[9] namely

$$\bar{\sigma}^2 = \bar{\sigma}_{\mathrm{M}}^2(1 + q_1^2 f^2) - 2q_1 f \bar{\sigma}_{\mathrm{M}}^2 \cosh\left(\frac{3}{2} q_2 \frac{\sigma_{\mathrm{m}}}{\bar{\sigma}_{\mathrm{M}}}\right) \tag{8}$$

A simplified form has been suggested by [10] and [11] in order to make the yield function amenable to analytic derivations especially in the presence of the added complexity due to anisotropy. This simplification is obtained by expanding the hyperbolic cosine term namely; $\cosh(3q_2\sigma_{\mathrm{m}}/\bar{\sigma}_{\mathrm{M}})$in terms of its power series. In many deformation processes $(3q_2\sigma_{\mathrm{m}}/\bar{\sigma}_{\mathrm{M}})$ is of a magnitude less than unity, hence, the suggested yield function derived from expression (8) is

$$\bar{\sigma}^2 = \bar{\sigma}_{\mathrm{M}}^2(1 - q_1 f)^2 - \frac{9}{4} f q_1 q_2^2 \sigma_{\mathrm{m}}^2 \tag{9}$$

where $\bar{\sigma}$ is given by Hill's non-quadratic yield function (5)

The inclusion of the parameters q_1 and q_2 are suggested by Tvergaard [9] in order to bring deformation of porous solids closer to experiments. It has been pointed out by several investigators e.g. [12,13] that q_1 and q_2 are set to be dependent on mean stress σ_{m} and hardening n, while q_2 also be dependent on void shape λ_1. This dependence is represented by semi-empirical relations as given for completeness in Appendix A.

Following the same derivation procedures given in ref. [10], a law for void growth is found after lengthy algebraic manipulation as

$$\frac{\mathrm{d}f}{\mathrm{d}\varepsilon_1} = \frac{9q_1q_2^2 f(1-f)\sigma_{\mathrm{m}}}{(2\bar{\sigma}^{(2-m)}/(1+\bar{r}))[-|2\sigma_3 - \sigma_1 - \sigma_2|^{m-1} + (1+2\bar{r})|\sigma_1 - \sigma_2|^{m-1}] + 3q_1q_2^2 f\sigma_{\mathrm{m}}} \tag{10}$$

The flow rule is derived based on the normality rule of the strain vector to the flow potential resulting in the expressions given in Appendix A. Specifically the strain along the direction identifying plane strain is given by

$$\mathrm{d}\varepsilon_2 = \mathrm{d}\lambda \left\{ \frac{\bar{\sigma}^{(2-m)}}{(1+\bar{r})} \left[-|2\sigma_3 - \sigma_1 - \sigma_2|^{m-1} - (1+2\bar{r})|\sigma_1 - \sigma_2|^{m-1} + \frac{3}{2} q_1 q_2^2 f \sigma_{\mathrm{m}} \right] \right\} \tag{11}$$

An expression governing the rate of change of the matrix effective strain may be also derived in the form

$$\frac{\mathrm{d}\bar{\varepsilon}_{\mathrm{M}}}{\mathrm{d}\varepsilon_{\mathrm{v}}} = \frac{4(1-q_1 f)^2}{9q_1q_2^2 f(1-f)\,(\sigma_{\mathrm{m}}/\bar{\sigma}_{\mathrm{M}})} \tag{12a}$$

where the volumetric strain increment is given by

$$\mathrm{d}\varepsilon_{\mathrm{v}} = \frac{\mathrm{d}f}{1-f} \tag{12b}$$

Note that all above formulas reduce to simplified Gurson–Tvergaard expressions for a Mises type matrix material when $m = 2$ and $\bar{r} = 1$ and to classical Mises function for $m = 2$, $\bar{r} = 1$ and $f = 0$.

During bending of a wide sheet metal the deformation mode is that of plane strain i.e. $d\varepsilon_2 = 0$. The stress system at the outer fiber is such that $\sigma_3 = 0$, $\sigma_2/\sigma_1 = \alpha$, $\sigma_{\mathrm{m}} = (1+\alpha)/3$ and

$$\frac{\sigma_1}{\bar{\sigma}} = \left[\frac{2(1+\bar{r})}{|1+\alpha|^m + (1+2\bar{r})|1-\alpha|^m} \right]^{1/m} \tag{13}$$

as may be found from the yield function (5). This results in further simplifications in expressions (11) and (10) so that

$$[|1+\alpha|^m + (1+2\bar{r})|1-\alpha|^m]^{((2/m)-1)} \left[(1+2\bar{r}) \frac{|1-\alpha|^{m-1}}{|1+\alpha|} - |1+\alpha|^{m-2} \right] = 2^{((2/m)-2)}(1+\bar{r})^{(2/m)} q_1 q_2^2 f \tag{14a}$$

$$\frac{\mathrm{d}f}{\mathrm{d}\varepsilon_1} = \frac{3q_1q_2^2 f(1-f)(1+\alpha)}{[2\bar{\sigma}^{(2-m)}/(1+\bar{r})][|1+\alpha|^{m-1} + (1+2\bar{r})|1-\alpha|^{m-1}] + f q_1 q_2^2 (1+\alpha)} \tag{14b}$$

Similar derivations may be made for orthotropic yield function (7) applied to plane strain conditions. For brevity the outcome of this derivation—without details are given as

$$\frac{\bar{\sigma}}{\sigma_1} = \{F_2[r_{90} + r_0\alpha^2 + r_0 r_{90}(1-\alpha)^2]\}^{1/2} \tag{15}$$

$$\alpha = \frac{1}{2}\left[\frac{2F_2 r_0 r_{90} - q_1 q_2^2 f/2}{F_2 r_0(1+r_{90}) + f q_1 q_2^2/4} \right] \tag{15a}$$

$$\frac{\mathrm{d}\varepsilon_1}{\mathrm{d}f} = \frac{F_2[r_0 r_{90}(1-\alpha) + 2r_{90}] + f q_1 q_2^2 (1+\alpha)/4}{3f(1-f)q_1 q_2^2 (1+\alpha)/4} \tag{15b}$$

where

$$F_2 = 3/2\,(r_0 + r_{90} + r_0 r_{90})$$

4. Failure conditions

Void growth with developing plastic deformation often ends by coalescence of neighboring voids leading to ductile fracture. Commonly accepted ductile failure criteria are based on consideration of internal necking in the ligaments of matrix material between voids. Two versions of this type of ductile failure criteria are applied in the present work. The first is due to Pardoen and Hutchinson (P&H) [12] and the second is suggested by Ragab (R) [14]. They are respectively given below

Condition 'P&H':

$$\frac{\sigma_1}{\bar{\sigma}_M} \geq \left[\frac{(0.1+0.27n+4.83n^2)}{\lambda_1^2}(b_2/b_1-1)^2+\frac{1.24}{\sqrt{b_1/b_2}}\right] \times [1-(b_1/b_2)^2] \quad (16a)$$

Condition 'R':

$$\frac{\sigma_1}{\bar{\sigma}_M} \geq \left[1+\frac{2\lambda_1^2}{(b_2/b_1-1)}\right]\log\left[1+\frac{(b_2/b_1-1)}{2\lambda_1^2}\right] \times \left[1-\frac{\pi}{4}\left(\frac{b_1}{b_2}\right)^2\right]\left(\frac{\varepsilon_l}{\varepsilon_1}\right)^n \quad (16b)$$

Another ductile failure phenomenon is related to localization of deformation into either bulk or surface shear bands. A first ductile failure condition developed by McClintock (Mc) [15] considers that deformation shifts from a homogeneous flow to that localized in shear bands joining ellipsoidal holes within a hardening matrix. This condition has been put by Ragab [11] in the following inequality.

Condition 'Mc':

$$\frac{1}{\bar{\sigma}_M}\frac{d\bar{\sigma}_M}{d\bar{\varepsilon}_M} \leq \frac{n}{\bar{\varepsilon}_M} \leq \sqrt{\frac{3}{8}(1+\lambda_1^2)}\left(\frac{f}{f_i}\frac{1-f_i}{1-f}\right)^{2/3}\left(\frac{\lambda_{1i}+1}{\lambda_1+1}\right)^2 \times \left(\frac{b_{1i}}{b_{2i}}\right)\exp\varepsilon_1 \quad (17a)$$

Another condition for the initiation of surface shear bands has been put by Hutchinson and Tvergaard (H&T) [16] and Valkonen et al. [17] for a power-law hardening material as Condition 'H&T':

$$n \leq \varepsilon_f[1-\exp(-2\varepsilon_f)] \quad (17b)$$

Note that the above condition was derived by considering the initiation of shear bands in plane-strain tension as a bifurcation phenomenon. In the present work ε_f in expression (17b) is viewed following McClintock [15] as the limit ligament strain ε_l (see Eq. (18b) below) within a shear band joining ellipsoidal voids.

To apply the above fracture conditions, the evolution of void shape with straining must be defined quantitatively. Reference [13] offered semi-empirical relations determining the current void aspect ratio λ_1 as being dependent on its initial aspect ratio λ_{1i}, mean stress σ_m, initial void volume fraction f_i and current strain ε_1. These semi-empirical relations are listed in Appendix A for an initially prolate or oblate void.

Furthermore several parameters appearing in Eqs. (16a), (16b) and (17a), (17b) pertaining to the evolution of void shape and its surrounding material are given in reference [14] for small values of void fractions as

$$\left(\frac{b_1}{b_2}\right)^3 \cong \frac{6f}{\pi\lambda_1}\exp(1.5\varepsilon_1), \quad \left(\frac{b_{i1}}{b_{2i}}\right) \cong \frac{6f_i}{\pi\lambda_{1i}} \quad (18a)$$

and

$$\varepsilon_l \cong 2\log\left[\left(\frac{1-b_2/b_1}{1-b_{2i}/b_{1i}}\right)\left(\frac{f/\lambda_1}{f_i/\lambda_{1i}}\right)^{1/3}\right] \quad (18b)$$

5. Method of solution

The objective of the solution is to estimate the failure strain ε_f at which the bendability of the sheet metal is exhausted. This is realized by solving the two differential Eqs. (10) and (12a) to obtain the current values of f and $\bar{\varepsilon}_M$ corresponding to a current value of ε_1. Initial values at $\varepsilon_1 = 0$ are $f = f_i$ and $\bar{\varepsilon}_M = 0$. Obviously the sheet properties n, $\bar{r}$ and m are to be specified. The current values of $(\bar{\sigma}_M/\bar{\sigma})$ and α are determined at each step from Eqs. (9) and (14a) respectively. With the progress of strain its limiting value ε_f is found by applying one of the ductile failure criteria given by Eqs. (16a), (16b) or (17a), (17b). The minimum value of (R_i/t_o) corresponding to ε_f and hence A_f in expression (3) defines the bendability of the sheet metal.

6. Results

As described by expressions (3) the bendability of the plate is governed by its ductility. The four suggested criteria for prediction of fracture strain as given by Eqs. (16a), (16b) and (17a), (17b) are used for typical sheet metal properties ($n = 0.2$, $\bar{r} = 1.0$ and m = 2) to predict ε_f and hence A_f which give the minimum bend radius ratio $(R_i/t_o)_{min}$ as plotted in Fig. 1. For realistic values of initial void volume fraction

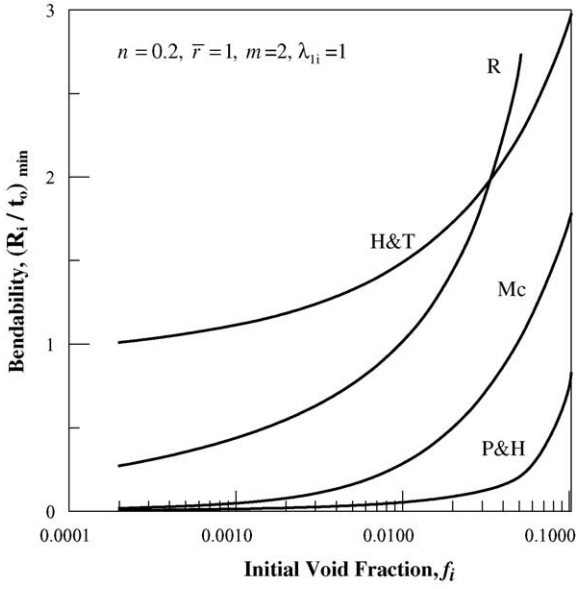

Fig. 1. Predictions of bendability $(R_i/t_o)_{min}$ for different initial void volume fractions by various ductile fracture conditions; P&H: Pardoen and Hutchinson [12], Mc: McClintock [15], H&T: Hutchinson and Tvergaard [16] and R: Ragab [14].

Table 1
Comparison among predictions of the two fracture conditions 'H&T' and 'R' for $n = 0.2$, $\bar{r} = 1$ and $\lambda_{1i} = 1$

Fracture condition	$f_i = 0.002$		$f_i = 0.05$	
	A_f	$(R_i/t_o)_{min}$	A_f	$(R_i/t_o)_{min}$
Shear band condition 'H&T'. Eq. (17b), [16]	0.291	1.01	0.124	3.31
Micro-necking condition 'R'. Eq. (16b), [14]	0.536	0.28	0.167	2.26

close to that observed in sheet metals; say ≈0.001, the conditions 'R' for internal micro-necking and 'H&T' for surface shear band formation predict values of $(R_i/t_o)_{min}$ in the same order of those known in industry [2]. The other two failure conditions namely 'P&H' and 'Mc' require much higher f_i values to predict reasonable $(R_i/t_o)_{min}$. The condition 'R' predicts almost zero value for $(R_i/t_o)_{min}$ for an initial $f_i \leq 10^{-4}$ which means that a clean sheet metal may be bent almost–as expected–over itself. Such comparison among failure conditions will be mostly limited in the next sections to one of internal necking and one to shear band namely**;** the 'R' and 'H&T' conditions respectively.

Table 1 shows a comparison among the predicted bendability $(R_i/t_o)_{min}$ and the reduction in area at fracture A_f according to the above two failure conditions. Each reduction in area corresponds to a selected f_i. The condition 'H&T' predicts smaller range of reductions in area corresponding to $0.002 < f_i < 0.05$.

The bendability of sheet metals is dependent on its width to thickness ratio; being better for narrower sheets. This is mainly related to the ductility of the outer fiber as a function of the degree of stress biaxiality; $\propto = \sigma_2/\sigma_1$. For narrow sheets the stress state is almost uniaxial $\propto = 0$, and ductility is higher than that for plane strain existing in wide sheets $\propto = 0.5$. This is demonstrated in Fig. 2 showing lower bendability (i.e. greater $(R_i/t_o)_{min}$) with increasing biaxiality as predicted by two fracture criteria. This is an outcome of faster void growth (as indicated by the dotted line in Fig. 2) and hence coalescence for higher mean stress $\sigma_m = \sigma_1 (1 + \propto)/3$ under plane strain condition.

The effect of sheet metal properties namely n and $\bar{r}$ (and hence m) are displayed in Figs. 3 and 4. The prediction of failure due to formation of surface shear bands is highly sensitive to the strain hardening of the metal as seen from condition (17b). Hence bendability becomes dependent on the value of n. This observation does not apply to predictions based on the failure condition pertaining to internal necking of microvoid material ligaments as shown in Fig. 3. The sensitivity to strain hardening is overestimated by the maximum bending moment condition given by expression (6) due to Leu [4]. Sheet metals with normal anisotropy i.e. $\bar{r} > 1$ possess lower bendability and vice versa as indicated by the predictions of Fig. 4 for the two failure conditions 'H&T' and 'R' as well as that of Wang et al [3]. Note that to obtain the results plotted in Fig. 4; the exponent m is set as $m = 2$ for $\bar{r} > 1$ and

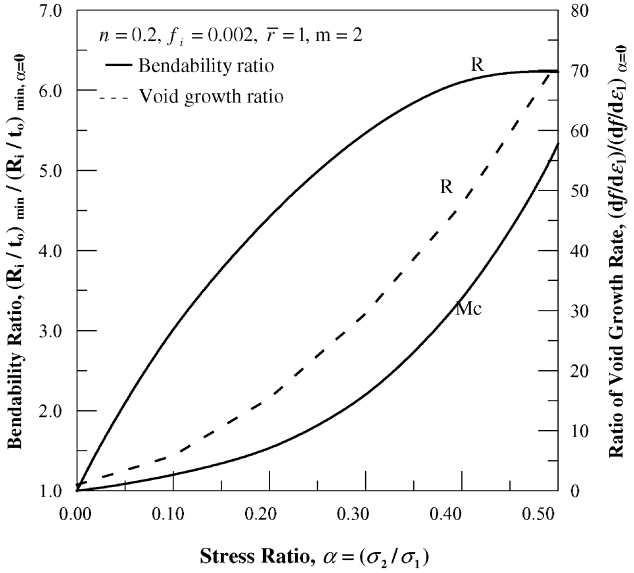

Fig. 2. Bendability $(R_i/t_o)_{min}$ vs. stress biaxiality ratio $\alpha = \sigma_2/\sigma_1$ as predicted by two failure conditions: internal necking failure condition 'R' [14] and shear band condition 'H&T' [16]. Also shown void growth rate vs. biaxiality ratio for the condition 'R'.

$m = 1 + \bar{r}$ for $\bar{r} < 1$. This is explained in view of expression (14) indicating a higher value for $\bar{r} > 1$; thus satisfying the fracture condition more promptly with smaller predictions of failure strain and hence lower bendability as seen from Fig. 4. The slight variation of bendability as predicted from the shear band condition 'H&T' (17b); results directly from the change of the exponent F in expression (4) rather than any variation in the predicted A_f which depends solely in this case on the strain hardening of the sheet metal.

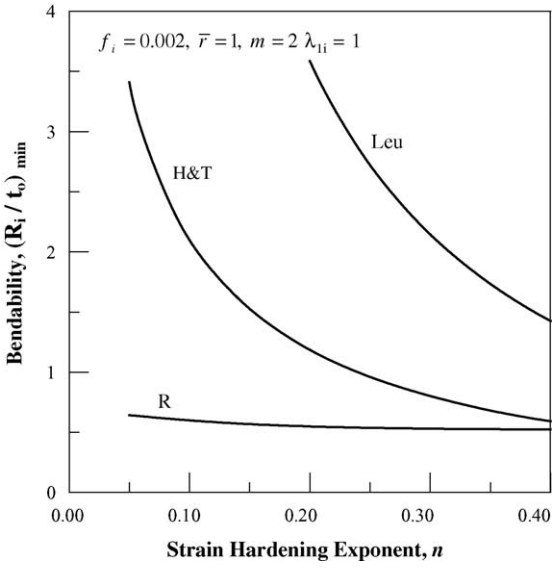

Fig. 3. Variation of bendability $(R_i/t_o)_{min}$ with strain-hardening exponent as predicted by three fracture conditions: internal micro-necking 'R' [14], shear band formation 'H&T' [16] and maximum bending moment 'Leu' [4].

Table 2
Comparison among bendability of steel sheets with isotropic, orthotropic anisotropy and nomal anisotropy and orthotropic anisotropy respectively, $n = 0.2$, $f_i = 0.005$, $\lambda_{1i} = 1$

Condition	ε_f	$(R_i/t_o)_{min}/(R_i/t_o)_{isotropic}$
Case1: Isotropic, $r_0 = r_{90} = 1$	0.413	1
Case2: Orthotropic anisotropy, rolling direction transverse to bend line, r_0 = H/G = 1.32, i_{90} = H/F = 1.68 [18]	0.389	1.09
Case3: Orthotropic anisotropy, rolling direction along bend line, r_0 = H/F = 1.68, r_{90} = H/G = 1.32 [18]	0.308	1.5
Case4: Normal anisotropy, $r_0, r_{90}, \bar{r} = [(H/G + H/F)]/2 = 1.5$	0.349	1.27

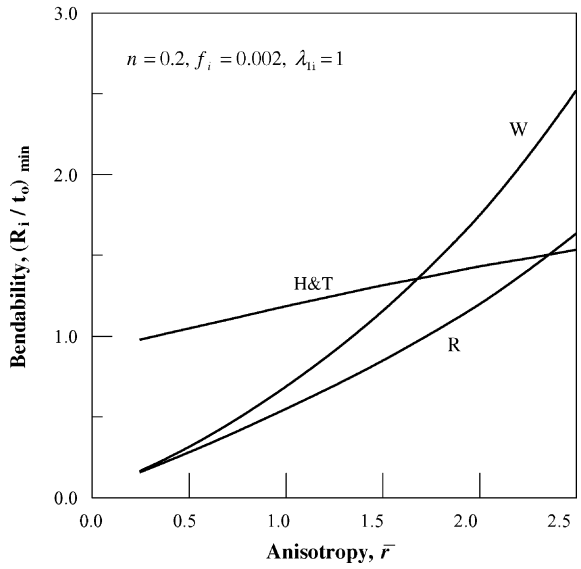

Fig. 4. Variation of bendability $(R_i/t_o)_{min}$ with normal anisotropy as predicted by three conditions: internal micro-necking 'R' [14], shear band formation 'H&T' [16] and Wang et al.' W' [3].

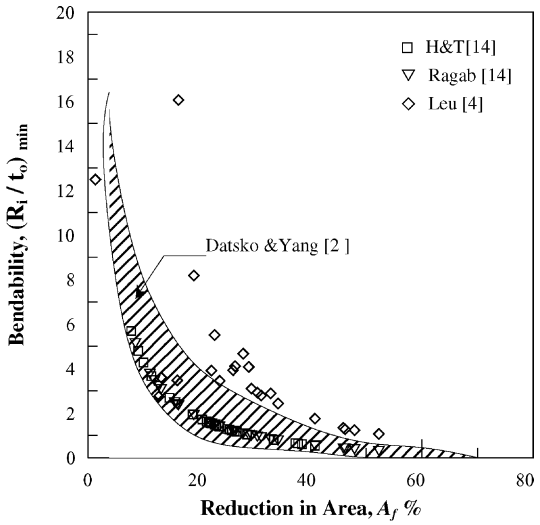

Fig. 5. Comparison of bendability $(R_i/t_o)_{min}$ as predicted according to three failure conditions with experiments [2]. The symbols refer to bendability of various sheet metals of properties as given in Appendix B.

In order to differentiate between bendability of an anisotropic sheet bent with its rolling direction either transverse (case 3 in Table 2) or along (case 4) to the bend line, resort has to be made to Hill's orthotropic yield expressions namely; (7), (15a) and (15b).

A typical cold rolled steel sheet properties are used such as H/G = 1.32 and H/F = 1.68 [18]. Table 2 indicates better bendability predictions for the sheet in case 2 than in case 3; as appreciated in industrial practice. Note that in case 4 which assumes planar isotropy predictions represent an average value for both cases 2 and case 3.

7. Comparison with experiments

Available bendability experiments for a large variety of materials were presented by Datsko and Yang [2]. In the form of $(R_i/t_o)_{min}$ versus the reduction in area at fracture A_f. No other material data such as hardening exponent, anisotropy etc were specified by them. However the hatched band in Fig. 5 represents the domain within which the experimental data of Datsko and Young lie. The bendability of various sheet metals for which the material properties are listed in Appendix B are predicted for a wide range of $0.05 < n < 0.45$, $0.37 < \bar{r} < 4.5$ and $1.37 \leq m \leq 2$. In view of lack of data concerning the initial void volume fraction f_i a value of 0.005 has been assumed for all alloys in Fig. 5.

The predictions of the two failure conditions 'R' and 'H&T' all lie within the experimental band unlike those calculated from the bendability condition of Leu [4], expression (6) indicating an obvious overestimation or say an upper limit.

8. Conclusions

The application of porous plasticity formulation to predict the bendability of sheet metals has confirmed the details of the empirical practice accepted in industry. The considered material model assumes the presence of initial micro-structural voids which grow in volume and change in shape with accumulating strain. Fracture due to either shear band formation or internal necking between neighboring voids yielded the required bendability-ductility curves. The results indicate better bendability for materials with higher strain hardening and small initial void fractions. Anisotropic sheet metals with the bend line oriented transverse to the rolling direction manifest better bendability than these with their bend line taken along the rolling direction. Predicted bendability according to a micro necking failure condition compares favorably with experimental evidence for a variety of sheet metal properties.

Appendix A

The dependence of the parameters q_1 and q_2 on (σ_m, λ_1, n) is suggested in refs. [12,13] to take the form

$$q_1 = A + B\left(\frac{\sigma_m}{\bar{\sigma}}\right) + C\left(\frac{\sigma_m}{\bar{\sigma}}\right)^2 + D\left(\frac{\sigma_m}{\bar{\sigma}}\right)^3$$

where $A = 2.275 - 3.549\ n + 3.837\ n^2$; $B = -0.918 + 1.320\ n - 0.316\ n^2$; $C = 0.529 - 2.310\ n + 2.354\ n^2$; $D = -0.098 + 0.269\ n + 0.701\ n^2 - 1.783\ n^3$

$$\text{Oblate voids}(\lambda_1 < 1): q_2 = \lambda_1^{\zeta_0} \quad \text{for} \quad \frac{1}{3} \le \left(\frac{\sigma_m}{\bar{\sigma}}\right) \le 2 \tag{A.1}$$

where $\zeta_o = [0.206 \log\left(\frac{\sigma_m}{\bar{\sigma}}\right) - 0.266] - 0.02\ n$

$$\text{Prolate voids}\ (\lambda_1 \ge 1):\ q_2 = \lambda_1^{\zeta_o} \quad \text{for} \quad \frac{1}{3} \le \left(\frac{\sigma_m}{\bar{\sigma}}\right) \le 2 \tag{A.2}$$

where

$$\zeta_p = \left[-3.484 + 11.614\left(\frac{\sigma_m}{\bar{\sigma}}\right) - 13.720\left(\frac{\sigma_m}{\bar{\sigma}}\right)^2 + 6.541\left(\frac{\sigma_m}{\bar{\sigma}}\right)^3 - 1.06\left(\frac{\sigma_m}{\bar{\sigma}}\right)^4\right] + 0.2n$$

For void shape evolution the following semi-empirical relations [13] (with slight modification) are used for the range $1/6 \le \lambda_{1i} \le 6$

Initially prolate void: $\lambda_{1i} \ge 1$, $1/3 < (\sigma_m/\bar{\sigma})$

$$\log(\lambda_1/\lambda_{1i}) = [(-0.535 + 0.0235 \sin\varepsilon) \log \lambda_{1i} + (2 - \sigma_m/\bar{\sigma}_M + n)](1 - f_i)(1.15 \sin\varepsilon) \tag{A.3}$$

$$\text{Initially oblate void}:\ \lambda_{1i} \le 1,\ \frac{1}{3} < \left(\frac{\sigma_m}{\bar{\sigma}}\right) < 3$$

$$\log(\lambda_1/\lambda_{1i}) = \left[\left(\frac{-\log\lambda_{1i}}{0.109 + 1.224\sin\varepsilon}\right) + \left(2 - \frac{\sigma_m}{\bar{\sigma}_M} + n\right)\right] \times (1 - f_i)(1.15\sin\varepsilon) \tag{A.4}$$

The validation of expressions (A.3) and (A.4) has been discussed in reference [13] indicating their close predictions compared to the extensive finite element solution due to Pardoen and Hutchinson [12].

The flow rule derived for simplified Gurson–Tvergaard flow function describing a matrix material obeying Hill non-quadratic anisotropic yield condition are obtained as

$$\begin{aligned}
d\varepsilon_1 &= d\lambda\left\{\frac{\bar{\sigma}^{(2-m)}}{(1+\bar{r})}\left[-|2\sigma_3 - \sigma_1 - \sigma_2|^{m-1} + (1+2\bar{r})|\sigma_1 - \sigma_2|^{m-1} + \frac{3}{2}q_1q_2^2 f\sigma_m\right]\right\}\\
d\varepsilon_2 &= d\lambda\left\{\frac{\bar{\sigma}^{(2-m)}}{(1+\bar{r})}\left[-|2\sigma_3 - \sigma_1 - \sigma_2|^{m-1} - (1+2\bar{r})|\sigma_1 - \sigma_2|^{m-1} + \frac{3}{2}q_1q_2^2 f\sigma_m\right]\right\}\\
d\varepsilon_3 &= d\lambda\left\{\frac{\bar{\sigma}^{(2-m)}}{(1+\bar{r})}\left[2|2\sigma_3 - \sigma_1 - \sigma_2|^{m-1} + \frac{3}{2}q_1q_2^2 f\sigma_m\right]\right\}\\
d\varepsilon_v &= d\lambda\left\{\frac{9}{2}q_1q_2^2 f\sigma_m\right\} = \frac{df}{(1-f)}
\end{aligned} \tag{A.5}$$

$$d\lambda = \frac{df}{\frac{9}{2}q_1q_2^2 f(1-f)\sigma_m} \tag{A.6}$$

Appendix B

See Table B.1.

Table B.1
properties of sheet metals as used in predicting bendability in Fig. 6

Alloy	n	$\bar{r}$
Steels		
DDQ	0.18	1.65
High Strength	0.18	0.95
Al–K	0.22	1.8
Rimmed	0.19	1.49
HSLA	0.18	1.2
Dual phase	0.16	1
Ti-stabilized	0.24	2
Interstitial free	0.3	2.5
Stainless Steels		
18-18 Aust.	0.48	1
409	0.2	1.2
18-8	0.433	0.84
Aluminums		
3003-0	0.23	0.6
Al–Mg	0.19	0.56
1100-0	0.25	0.62
203	0.18	0.78
Pure	0.24	0.86
Cold rolled	0.04	0.76
Al–Mn	0.24	0.66
Al–Mg–Si	0.28	0.74
Al–Cu–Mg	0.14	0.74
Coppers		
Pure Cu	0.44	0.9
70/30 Brass	0.42	0.85
Cu–Ni	0.35	0.8
Others:		
Ti alloys	0.05	3
Zn alloys	0.1	0.5
Zirc alloy	0.12	4.5
Zn–Ti	0.05	0.37

References

[1] Metals Handbook, vol.4, American Society for Metals, Metals Park, Ohio.
[2] J. Datsko, C.T. Yang, ASME (November 1960) 309–314.
[3] C. Wang, G. Kinzd, T. Altan, J. Mater. Process. Technol. 39 (1993) 279–304.
[4] D.-K. Leu, J. Mater. Process. Technol. 66 (1997) 9–17.
[5] O. Hoffman, G. Sachs, Theory of Plasticity, McGraw-Hill, N.Y., 1953.
[6] A.R. Ragab, A.T. Abbas, ASME: J. Eng. Mater. Technol. 108 (1986) 250–257.
[7] R. Hill, Math. Proc.Cambridge Philos. Soc. 85 (1979) 179–191.
[8] R. Hill, The Mathematical Theory of Plasticity, Oxford University Press, Oxford, England, 1950.
[9] V. Tvergaard, Int. J. Fract. 18 (1982) 237.
[10] A.R. Ragab, Ch. A.R. Saleh, Int. J. Plast. 15 (1999) 1041–1065.
[11] A.R. Ragab, Ch A.R. Saleh, Mech. Mater. 32 (1999) 71–84.
[12] T. Pardoen, J.W. Hutchinson, J. Mech. Phys. Solids 48 (2000) 2467–2512.
[13] A.R. Ragab, Eng. Fract. Mech. 77 (2004) 1515–1534.
[14] A.R. Ragab, Acta Mater. 52 (2004) 3997–4009.
[15] F.A. McClintock, On the Mechanics of Fracture from Inclusions, in: Ductility, ASM, Metals, Park, OH, 1968.
[16] J.W. Hutchinson, V.T. Tvergaard, Int. J. Mech. Sci. 22 (1980) 339.
[17] A. Valkonem, A. Chatterjee, J.P. Hirth, Int. J. Mech. Sci. 29 (1987) 219–227.
[18] A.N. Bramley, P.B. Mellor, Int. J. Mech. Sci. 8 (1966) 101.